Application of SVM, ANN, GRNN, RF, GP and RT models for predicting discharge coefficients of oblique sluice gates using experimental data

Farzin Salmasi, Meysam Nouri, Parveen Sihag and John Abraham

ABSTRACT

Gates are commonly used to adjust water flow in open channels. By using an oblique/inclined gate, the water transferring capacity of open irrigation canals can be increased. Investigation of free and submerged discharge coefficients for inclined sluice gates is the focus of the present study. First an experimental apparatus incorporating an inclined gate was created. The inclined angle (β) and gate opening (a) were experiment variables, and the five inclination angles include: 0° (vertical gate), 15°, 30°, 45° and 60°. Experimental results showed a greater convergence of flow lines under the gate and increasing the gate angle causes the discharge coefficient to increase. Also experiments showed that increasing the submergence rate (y_t/a), decreases the inclined gate discharge coefficient. Performance metrics were created for the experimental results. The metrics utilized Gaussian process (GP) regression, support vector machine (SVM), artificial neural networks (ANN), generalized regression neural network (GRNN), random forest (RF) regression and random tree (RT) based models which were used to predict discharge coefficients (C_d) in both submerged and free flow conditions. The model input parameters were the ratio of the upstream water depth to gate opening (y/a) and the inclined angle (β) for free flow and also the submergence rate (y_t/a) for submerged flow. The prediction models show that the ANN model in free flow conditions has the following performance metrics: Coefficient of determination, $R^2 = 0.9957$, Root Mean Square Error (RMSE) = 0.0044, and Mean Absolute Error (MAE) = 0.0017. The performance metrics for submerged flow conditions were $R^2 = 0.9922$, RMSE = 0.0079 and MAE = 0.0054. The ANN approach is the most accurate model compared to the others.

Key words | artificial intelligence, discharge coefficient, free flow, inclined sluice gate, submerged flow

Farzin Salmasi (corresponding author)
Department of Water Engineering, Faculty of Agriculture,
University of Tabriz,
Tabriz,
Iran
E-mail: *salmasi@tabrizu.ac.ir*

Meysam Nouri
Department of Water Engineering, Faculty of Agriculture,
University of Urmia,
Urmia,
Iran

Parveen Sihag
Department of civil Engineering,
Shoolini University,
Solan, Himachal Pradesh,
India

John Abraham
School of Engineering,
University of St. Thomas, Minnesota,
2115 Summit Avenue St. Paul, Minnesota 55105,
USA

HIGHLIGHTS

- Investigation of the free and submerged discharge coefficients (C_d) for inclined sluice gates is the focus of the present study.
- The inclination angle and gate opening were experiment variables.
- Experimental results showed increasing the gate angle causes C_d to increase.
- Increasing submergence rate, decreases the inclined gate C_d.
- Six models were used to predict C_d in both submerged and free flow conditions.

NOTATION

Q	sluice gate discharge (m^3/s)	y	flow depth on upstream side of the sluice gate (m)
a	sluice gate opening (m)	y_t	tail water depth (m)

doi: 10.2166/ws.2020.226

g gravitational acceleration
C_d discharge coefficient of the gate
β normal inclination of the plane of the gate

INTRODUCTION

Flow discharge measurement is important for water resource management, especially in irrigation and environment engineering. Water is considered to be a scarce commodity in many countries and water use needs to be properly managed. Usually canals are used to transfer irrigation water. In these canals, sluice gates are often used for flow control and water measurement. The sluice gate discharge (Q) can be written as (Henry 1950):

$$Q = C_d a b \sqrt{2gy} \quad (1)$$

where C_d is the gate discharge coefficient, a is the gate opening, b is the canal width, y is the upstream water depth, and g is gravitational acceleration.

Rectangular vertical sluice gates have been studied by many researchers in the past. Henry (1950) presented a graph for discharge coefficient variation with y/a in free flow conditions and against y/a and y_t/a for submerged flow, where y_t is the tail water depth. Later, Rajaratnam & Subramanya (1967a) confirmed the Henry (1950) work and studied both free and submerged flows through a vertical gate (Rajaratnam & Subramanya 1967b). Based on Henry (1950), Swamee (1992) presented equations for free and submerged flow discharge coefficients. In this research, a criterion for free flow was presented. Ramamurthy *et al.* (1978) experimentally studied sluice gates with cylindrical edges in submerged flow conditions and high discharge coefficients were reported. Swamee *et al.* (2000) presented equations for determining sluice gate free flow discharge coefficients based on y/a. They provided an equation that can be used to calculate submerged flow discharge coefficients.

Lorenzo *et al.* (2009) investigated gates under submerged flow conditions; in that work, nearly 16000 field measured data points were obtained. This research demonstrated that discharge coefficients are a parabolic function of the gate opening (a). In another study, based on momentum and energy conservation between the upstream pool and contraction section, a new theoretical study for contraction coefficient calculation was presented by Belaud *et al.* (2009). That research provided contraction coefficient equations that can be used to quickly estimate discharge.

More recent investigations have been performed related to gates, such as Abdelhalim (2016); Bijankhan *et al.* (2013); Bijankhan & Kouchakzadeh (2014); Cassan & Belaud (2012); Habibzadeh *et al.* (2011); Salmasi *et al.* (2019); Silva & Rijo (2017); Bijankhan & Ferro (2018); Wu & Rajaratnam (2015), Nouri & Hemmati (2020) and interested readers are directed there for a comprehensive review of the science.

Daneshfaraz *et al.* (2016) used different kinds of gate edges to investigate the effect of the edge shape on flow. They reported variations of the contraction coefficient, discharge coefficient and pressure distribution according to different edge shapes.

Using an inclined gate, the water transferring capacity in irrigation canals can be increased. In other words, by increasing of the inclination angle, more water can pass through a canal and less backwater will occur. The irrigation canals can be made with short walls and this is important for determining the economic benefits of inclined gates.

Multivariate data analysis techniques such as artificial intelligence (AI) models and soft computing techniques have been employed for decision-support in water science (Al-Khatib & Gogus 2014; Roushangar *et al.* 2017; Akbari *et al.* 2019; Bahrami *et al.* 2019; Jahanpanah *et al.* 2019; Seyedzadeh *et al.* 2019). The operational costs and the time required for instrumentation is reduced by the development of predictive models which are integrated into decision-support systems (Brandhorst *et al.* 2017; Salmasi & Nouri 2017; Maroufpoor *et al.* 2019). In other words, because of high uncertainty, complexity of the solutions, and the large number of effective parameters and their interactions, these techniques can be used as a direct method to solve the problems (Seyedzadeh *et al.* 2019).

Artificial neural networks and support vector machines were used by Norouzi *et al.* (2019) for estimation of trapezoidal labyrinth weir discharge coefficients. According to the results from that study, a multilayer perceptron (MLP) network model provided superior results.

Despite the above studies, flow under an inclined gate has not been considered, even though this hydraulic structure can be used for upstream water level adjustment, as a measuring device, back water controller and for other

hydraulic applications. So, analysis of such a gate and its advantages is important to irrigation science. An experimental study of free and submerged flows under an inclined sluice gate is the main goal of this research. For each gate opening, the studied angles were 0° (vertical gate), 15°, 30° and 45°. Further, based on experimental results, Gaussian process (GP) regression, support vector machine (SVM), artificial neural networks (ANN), generalized regression neural network (GRNN), random forest (RF) regression and random tree (RT) are used to estimate both submerged and free flow discharge coefficients. This is the first investigation of the ability of the aforementioned techniques to predict discharge coefficients for inclined gates.

Increasing the discharge coefficient in hydraulic structures like types of gates (sluice or radial) and weirs in irrigation canals has been a focus in the scientific literature. More conveyance of water through these hydraulic structures can facilitate a decrease in the sizes of these structures or a reduction in freeboard in irrigation canals. Freeboard refers to the vertical distance between the top of the canal bank and the water surface at the design discharge. It provides safety against canal overtopping because of waves in the canal or unintentional raising of the water level which may be a result in closed/unclosed gates.

Governing equations

For inclined sluice gates, the discharge coefficient is a function of free and submerged flow conditions. Therefore, for determining the discharge coefficient, an explicit equation using input parameters a and y for free flow and y, a, and y_t for submerged flow conditions is obtained, as shown here:

$$c_d = f(a, y) \tag{2}$$

$$c_d = f(a, y, y_t) \tag{3}$$

The gate shape, upstream water level, surface tension, viscosity, Froude number, Reynolds number and inclination angle are the most important parameters that govern the discharge coefficients. In this experimental study, when the inclined gate was installed in an experimental flume, uniform flow conditions were not produced and flow lines converge rapidly compared with the vertical gate case. Figure 1 shows the flow pattern for this type of gate and it is seen that β is a new parameter that has been added to Equations (1) and (2):

$$c_d = f(a, y, \beta) \tag{4}$$

$$c_d = f(a, y, y_t, \beta) \tag{5}$$

EXPERIMENTAL FACILITIES

The experiments were performed in a rectangular flume 0.2 m and 0.65 m in width and depth, respectively. The lower edge of the sluice gate was cut with a 45° angle. For investigating the inclined angle, four angles – 0° (vertical gate), 15°, 30° and 45° – were used. Also, for each of these angles, five different gate openings – 10, 20, 30, 40, and 50 mm – were used. Figure 2 shows the experimental flume and location of the inclined gate. To achieve uniform and smooth flow upstream of the experimental section, flow straightening tubes were used. The upstream and downstream flow depth were measured using a ruler to an accuracy of ±0.1 mm. A sharp crested triangular weir at the upstream end of the flume was used to measure discharge.

APPLIED INTELLIGENT MODELS

For predicting discharge coefficients based on the experimental results, six artificial intelligence approaches were used: GP, SVM, ANN, GRNN, RF and RT. These methods will now be discussed in some detail.

Gaussian process (GP) regression

Classification and regression problems are two major parts of supervised learning methods. Among different kinds of approaches, Gaussian process regression is one of the most attractive supervised learning nonparametric approaches to predictions (Seeger 2004; Williams & Rasmussen 2006; Shi & Choi 2011; Kang *et al.* 2015). Considering a data set $\omega = \{(x_i, y_i) \mid i = 1,\ldots,n\}$, $x \in R^d$ is a d-dimensional input vector space and $y \in R$ is an output in a 1-dimensional vector space. In the regression approach, the conditional distribution of outputs due to specific inputs is important for understanding the relationship between inputs and outputs. In the Gaussian process, a joint Gaussian distribution covers a set of random

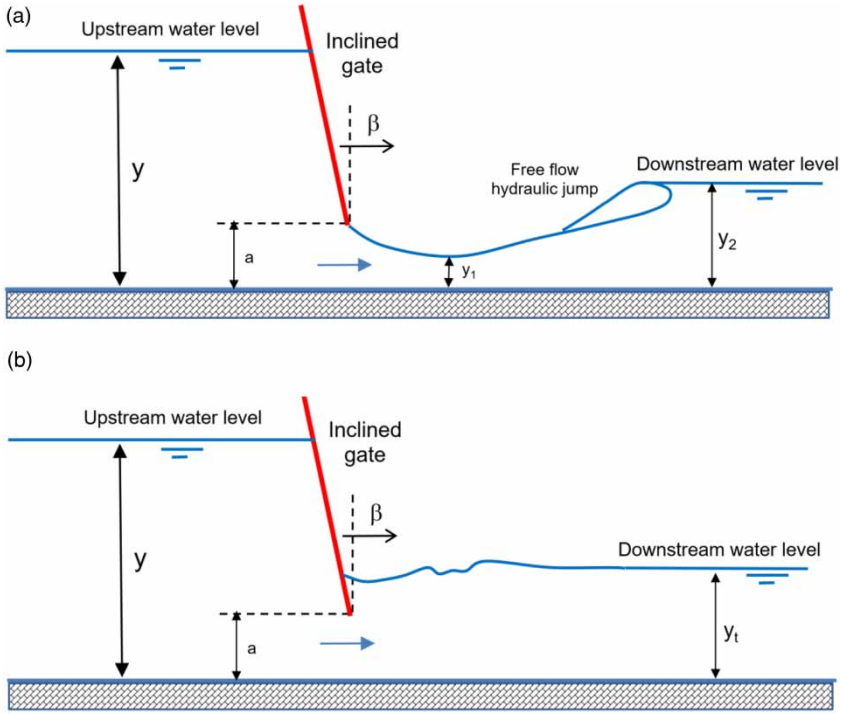

Figure 1 | Free (a) and submerged (b) flow in oblique/inclined sluice gate.

variables with a finite number. The Gaussian process $f(x)$ can specify the mean and covariance functions:

Mean function $m(x)$: $m(x) = E[f(x)]$

Covariance function or kernel function $K(x,x')$: $K(x,x') = [(f(x) - m(x))(f(x') - m(x'))]$.

For $x \in R^d$, with K_{ij} (x_i, x_j) $i,j = 1,\ldots,n$ for all pairs of $x \in R^d$ could make $K(X,X)$ the covariance matrix.

Support vector machine (SVM)

SVM is a soft computing approach that has been applied to many applications such as regression, classification, and forcasting. Cortes & Vapnik (1995) showed a kernel function which is useful for nonlinear regression. For a data set $\omega = \{(x_i,\ y_i) \mid i = 1,\ldots,n\}$ where $x \in R^d$ is a d-dimensional input vector space and $y \in R$ is an output in a 1-dimensional vector space, SVM regression can estimate the relationship between x and y. In the SVM approach the risk function is minimized by minimizing both empirical risk and $\|w\|^2$.

$$R = \frac{1}{2}\|w\|^2 + C_C \sum_{x_i} l_\varepsilon\ (y_i - f(\vec{x_i})) \tag{6}$$

where $\|w\|$ is a regression data vector, l_ϵ is a loss function that presents the difference between y_i (real output) and $f((\vec{x_i}))$ and C_C is a positive constant value needed to fix the prior. l_ϵ $(y_i - f((\vec{x_i}))$ will be 0 for $|y_i - f((\vec{x_i}))| < \epsilon$. otherwise it is equal to $|y_i - f((\vec{x_i}))|$. Minimizing the risk function can be accomplished with the following function:

$$f(x, \alpha, \alpha^*) = \sum_{i=1}^{l} (\alpha_i^* - \alpha_i)(\varphi(x_i), \varphi(x)) + b \tag{7}$$

where $\alpha_i^* \alpha_i = 0$ and $\alpha_i^*, \alpha_i \geq 0$, $(\varphi(x_i), \varphi(x))$ is an inner product kernel function and b is a bias term (Vapnik *et al.* 1996) and (Wang 2005).

Artificial neural networks (ANNs)

ANNs are widely used for numerical analysis and grouping (Sihag 2018; Jahani & Mohammadi 2019; Moazenzadeh & Mohammadi 2019). ANN-based models are biologically inspired and are composed of elements operating in parallel and arranged in patterns reminiscent of biological neural networks. They include three essential layers (the

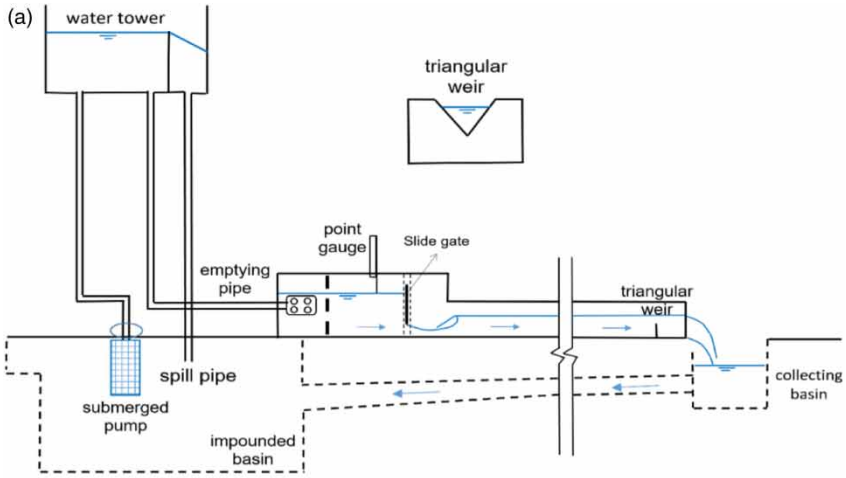

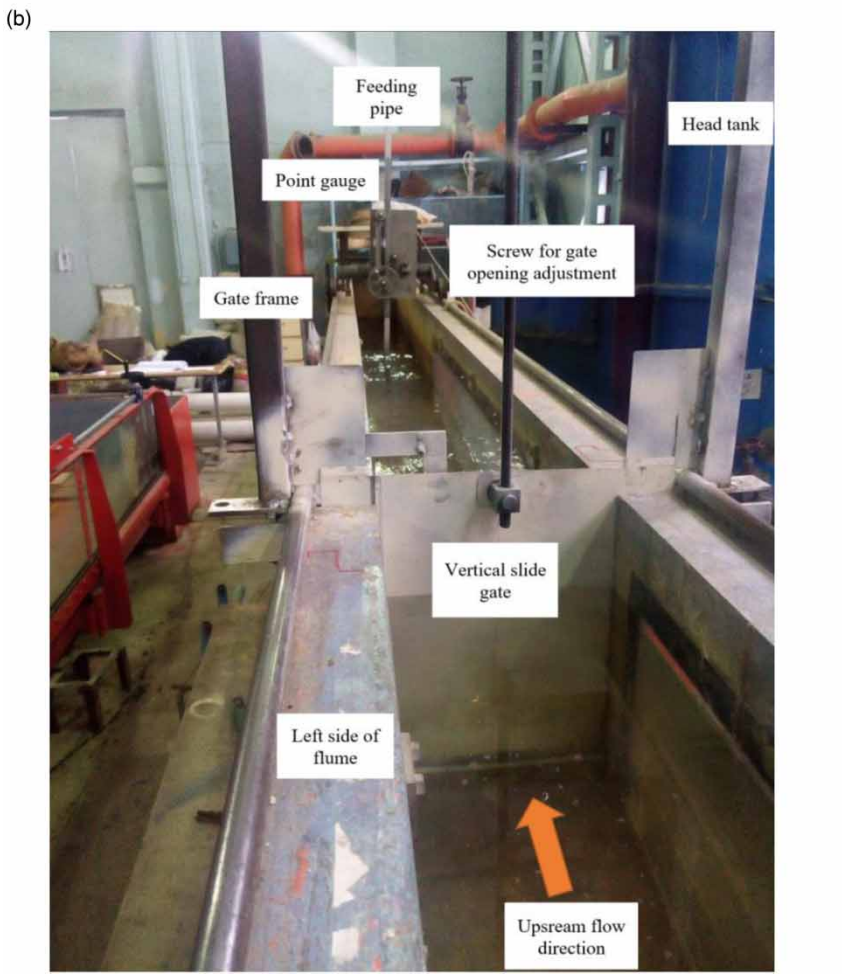

Figure 2 | The experimental setup. (a) Schematic of experimental setup. (b) Flow in a 10 m flume along with installed vertical gate.

information layer, the hidden layer, and the output layer). The channel in the midst of the layers is used to weight relationships in the midst of the hubs. Each node is similar to a biological neuron and performs mostly two tasks, encompassing information values and the weights related to each interaction. Its summation yields the activation function. The system creates a result which exists close to the watched target result. More details about ANNs are given by Simon (1999) and interested readers are directed there. In this current investigation, a single hidden layer is used for the model development.

Generalized regression neural network (GRNN)

A GRNN was first presented in Specht (1991) as a standardized radial basis function (RBF) network in which there is a hidden segment. These RBF segments are known as 'parts' and are used for instance in SVM and GP analysis. The main considerations are the widths of the RBF function. The GRNN model contains just four levels. Information components are in the first level, the subsequent level has the example components. Yields of this level are passed on to the summation components in the third level, and the last level covers the yield components. The primary level is totally connected to the second, pattern level, where every component shows a preparation example and its yield is a portion of the separation of the contribution from the stored examples. The ideal estimation of a GRNN parameter is determined by a trial and error process. For more information about GRNN, users are referred to Specht (1991) and Wasserman (1993).

Random forest (RF) regression

Random forest is one of the most recent methods utilized for grouping and regression-based calculations; the technique consists of several decisions *trees*. It uses arbitrary and bagging features when developing every *tree* to develop an uncorrelated *forest* whose estimation (on the whole group) is more precise than that of any single *tree*. In this method, quantity trees were utilized for determining or estimating an output. Tree indicators utilized numerical qualities randomly assigned to class names in a random forest classifier (Breiman 1999). RF regression utilizes a gathering of information parameters or self-assertively picks parameters at every node to grow a tree. The RF regression method requires just two specific characterizing parameters, for example, the number of parameters at every node and the quantity of trees (Breiman 1999).

Random tree (RT)

RT is a supervised machine learning technique; it is an ensemble learning algorithm that develops several individual trainers. Bagging is employed to construct an arbitrary set of data for developing decision trees. No pruning is carried out in RT. With back fitting, it permits estimation of class probabilities or output means in a relapse case. When utilizing this technique, two significant parameters are picked to be specific: the tallness h of the random tree and the number N of base classifiers (Kalmegh 2015).

Soft computing and goodness of fit assessment parameters

Regression and soft computing techniques models (i.e. GP, SVM, ANN, GRNN, RF and RT) were evaluated against actual values for their ability to predict the discharge coefficient (C_d). For the model goodness of fit assessment, three statistical parameters, namely, Coefficient of determination (R^2), Root Mean Square Error (*RMSE*), and Mean Absolute Error (*MAE*), were selected. The above-mentioned goodness of fit assessment parameters can be calculated by the following equations (Nouri & Hemmati 2020):

$$R^2 = \frac{n\sum AP - (\sum A)(\sum P)}{\sqrt{n(\sum A)^2 - (\sum P)^2}\sqrt{n(\sum A - \sum P)^2}} \tag{8}$$

$$\mathrm{RMSE} = \sqrt{\frac{1}{\mathrm{n}}\left(\sum_{\mathrm{i}=1}^{\mathrm{n}}(\mathrm{A}-\mathrm{P})^2\right)} \tag{9}$$

$$MAE = \frac{1}{n}|A - P| \tag{10}$$

where A and P are the measured and predicted discharge coefficients, respectively, and n is the total number of measured discharge coefficients. The perfect value for R^2 is unity and for MAE and RMSE, it is zero.

RESULTS AND DISCUSSION

Experimental results

Figure 3 shows the discharge coefficient variations against y/a for all the studied gate angles in free flow conditions. According to Figure 3, increasing the gate angle for a specified y/a causes the discharge coefficient to increase. Greater convergence of the flow lines under the inclined gate is the reason for this increase. As can be seen in Figure 3, at lower values of y/a, the effect of gate inclination angle on the discharge coefficient is insignificant and by increasing y/a, the effect of gate inclination angle increases. By increasing the gate inclination angle from 0° to 60°, the discharge coefficient increases considerably and there is no reduction in the discharge coefficient increasing by increase of the inclination angle.

The vertical gate ($\beta = 0$) discharge coefficients for submerged flow conditions are presented in Figure 4. By increasing of the submergence rate (y_t/a), the discharge coefficient decreases. The discharge coefficient values converge to 0.53 for large values of y/a. As can be seen in Figure 4, the effect of y_t/a, particularly at the lowest values of y/a, is considerable. By increasing y/a, the effect of y_t/a becomes insignificant.

Figure 5 shows the submerged inclined gate ($\beta = 15°$) discharge coefficient versus y/a for different values of y_t/a. The discharge coefficient converges to 0.57. As seen in Figure 5, the effect of inclination angle on the gate discharge coefficient in submerged flow conditions is clear and the same as flow free conditions; increasing the inclination angle with submerged flow conditions leads to an increase in the gate discharge coefficient.

Selecting and division of data

The experimental study is divided into two parts: free flow and submerged flow conditions. For the inclined gate structure, because of its special geometric shape, the most effective parameters include y/a and β for free flow and y/a, y_t/a and β for the submerged case. Previous studies on the other types of gates have demonstrated that upstream water level and gate openings can also play a key role in gate hydraulics (Parsaie *et al.* 2017; Parsaie *et al.* 2019).

In order to achieve acceptable results and an assessment of the model efficiency, the data set is divided into two independent blocks: testing and training sections. The training data is used to establish the model and the testing data is used to evaluate model accuracy. K-fold cross validation was used to avoid over-fitting (Cios *et al.* 2007; Shiri *et al.* 2015, 2019; Seyedzadeh *et al.* 2019). For free flow, the training data set included 68% of the available data (178 samples) and the testing utilized the remaining 32% (82 samples). For the submerged flow,

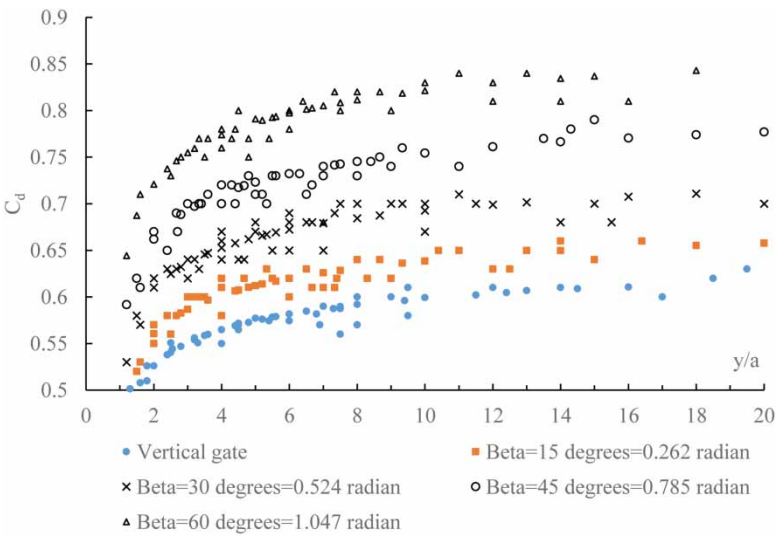

Figure 3 | Inclined gate free flow discharge coefficient variations.

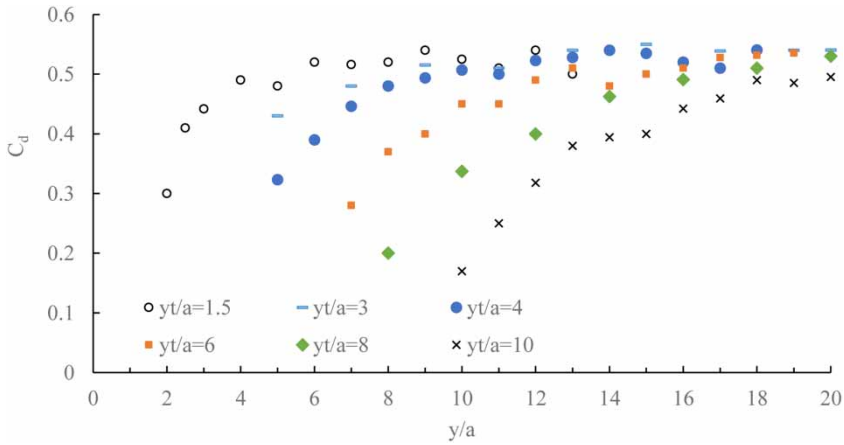

Figure 4 | Submerged vertical gate discharge coefficients.

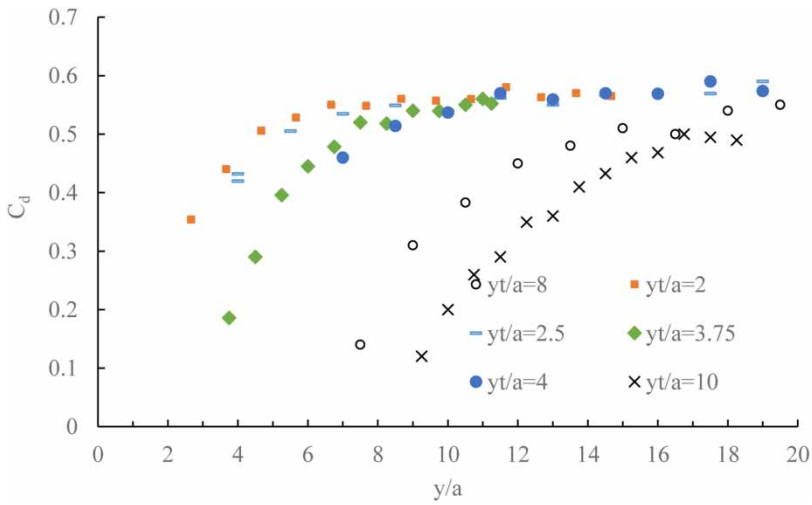

Figure 5 | Submerged inclined gate ($\beta = 15^{\circ}$) discharge coefficients.

Table 1 | Statistics related to the prediction of discharge coefficients (C_d) for free flow conditions

	Training data set			Testing data set		
Range	**y/a**	***B* (deg.)**	**C_d**	**y/a**	**β(deg.)**	**C_d**
Mean	8.2333	21.9944	0.6460	8.1911	23.5976	0.6495
Standard Deviation	6.5534	16.9607	0.0665	6.8055	16.5043	0.0664
Kurtosis	2.3476	−1.3844	−0.7658	2.0616	−1.2983	−0.4115
Skewness	1.6539	0.0490	0.1474	1.6135	−0.1050	0.0552
Minimum	1.2000	0.0000	0.5009	1.2000	0.0000	0.4701
Maximum	30.0000	45.0000	0.7866	30.0000	45.0000	0.7852
Confidence Level (95.0%)	0.9694	2.5088	0.0098	1.4953	3.6264	0.0146

the training included 68% of the available data (505 samples) and testing the remaining 32% (236 samples). The statistics of the input and output variables used for predicting the discharge coefficients (C_d) are listed in Tables 1 and 2. Furthermore, uncertainty with 95% confidence levels (Gueymard 2014; Behar *et al.* 2015; Maroufpoor *et al.* 2019) was used to gather more information on the effectiveness of the model performance.

Table 2 | Statistics related to the prediction of discharge coefficients (C_d) for submerged flow conditions

	Training data set				Testing data set			
Range	**y/a**	**y_t/a**	**β (deg.)**	**C_d**	**y/a**	**y_t/a**	**β (deg.)**	**C_d**
Mean	9.4427	3.2156	21.2673	0.5058	9.4674	3.0980	22.6907	0.5067
Standard Deviation	5.4940	2.2299	17.5107	0.0888	6.1502	2.1562	17.1993	0.0878
Kurtosis	1.3017	1.4758	−1.4713	2.8757	1.4214	2.3524	−1.4212	2.8724
Skewness	1.2057	1.4492	0.0642	−1.7090	1.3742	1.6444	−0.0570	−1.6831
Minimum	2.0000	1.1000	0.0000	0.1720	2.0000	1.1000	0.0000	0.1871
Maximum	30.0000	10.0000	45.0000	0.6197	29.0000	10.0000	45.0000	0.6185
Confidence Level (95.0%)	0.4803	0.1950	1.5309	0.0078	0.7887	0.2765	2.2057	0.0113

Table 3 | Comparison of soft computing based models for predicting C_d in free flow

	Training data set			Testing data set		
Models	**R^2**	**RMSE**	**MAE**	**R^2**	**RMSE**	**MAE**
GP_PUK	0.9943	0.0050	0.0027	0.9882	0.0072	0.0034
GP_RBF	0.9800	0.0094	0.0062	0.9757	0.0103	0.0066
SVM_PUK	0.9918	0.0062	0.0018	0.9881	0.0075	0.0022
SVM_RBF	0.9722	0.0116	0.0046	0.9708	0.0120	0.0049
ANN	0.9979	0.0030	0.0016	0.9957	0.0044	0.0023
GRNN	0.9997	0.0011	0.0005	0.9928	0.0058	0.0018
RF	0.9986	0.0026	0.0012	0.9906	0.0068	0.0029
RT	0.9996	0.0013	0.0009	0.9917	0.0065	0.0033

Table 4 | Single factor ANOVA results for free flow conditions

Source of Variation	**F**	***P*-value**	**F crit**	**Variation in groups**
Between actual and GP_PUK	0.0000	0.9991	3.8995	Insignificant
Between actual and GP_RBF	0.0005	0.9819	3.8995	Insignificant
Between actual and SVM_PUK	0.0142	0.9051	3.8995	Insignificant
Between actual and SVM_RBF	0.1116	0.7388	3.8995	Insignificant
Between actual and ANN	0.0000	0.9981	3.8995	Insignificant
Between actual and GRNN	0.0019	0.9655	3.8995	Insignificant
Between actual and RF	0.0173	0.8955	3.8995	Insignificant
Between actual and RT	0.0338	0.8544	3.8995	Insignificant

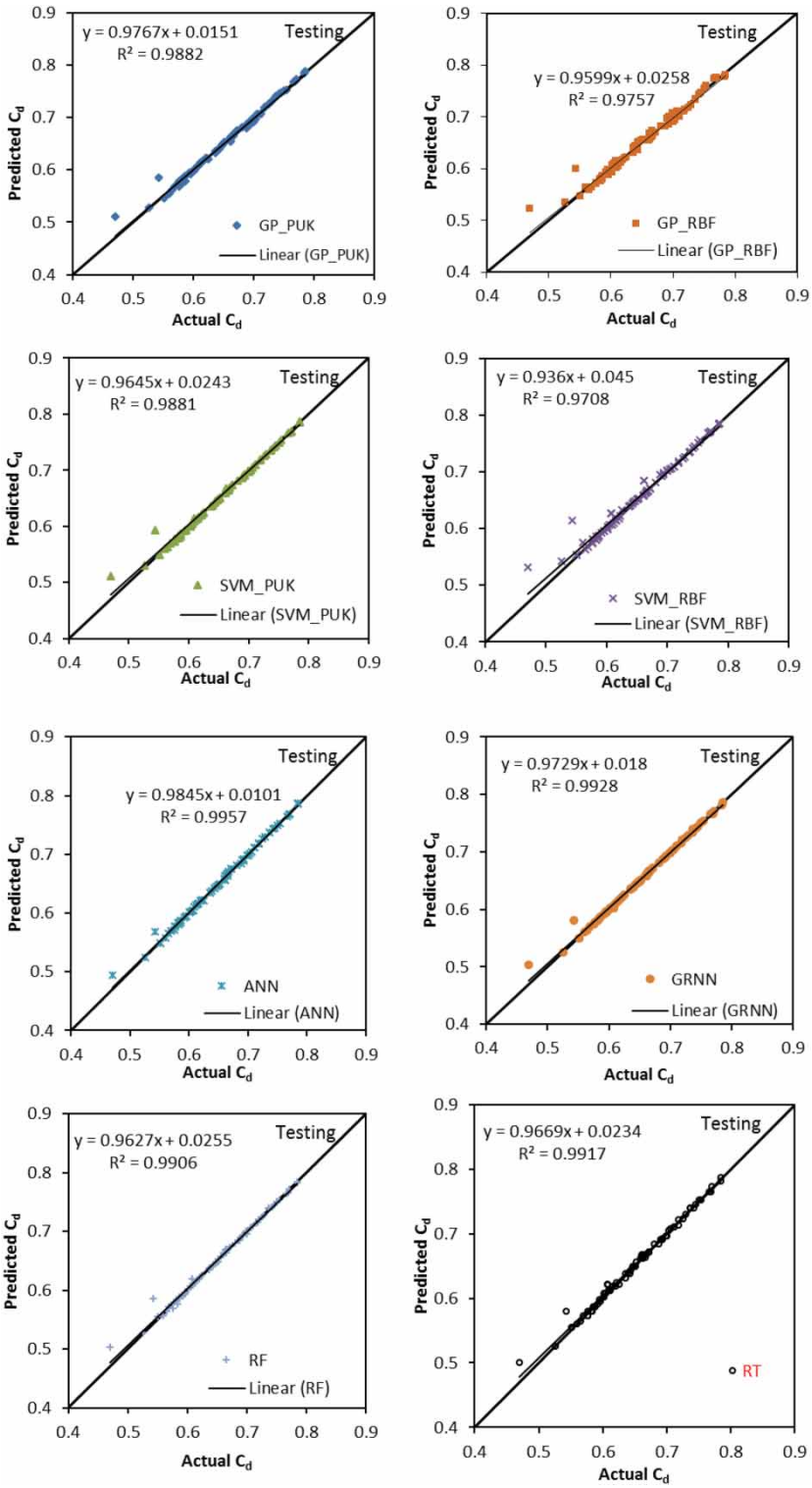

Figure 6 | Agreement plot from actual and predicted values of C_d for free flow using various soft computing techniques (testing stage).

Application of GP, SVM, ANN, GRNN, RF, and RT for estimating inclined gate free flow discharge coefficients (C_d)

Normally, the performance evaluation of GP, SVM, ANN, GRNN, RF and RT based models is done via *R2*, RMSE and MAE. Table 3 depicts the comparison of performance evaluation parameters for the predicted values. The higher values of *R2* and lower values of RMSE and MAE confirm model performance. If the *R2* value is 1 and RMSE and MAE values are zero then the model is ideal for predictions. For free flow conditions, the Pearson VII kernel function based on the GP and SVM models work better than radial basis function (RBF) kernel based models in the training and testing stages. For ANN and GRNN based models, the GRNN approach works better than the ANN-based approach in the model development stage whereas in the testing stage, ANN models work better than the GRNN approach. A comparison of RF and RT based models (Table 3) suggests that RT-based models work better than RF-based models with R^2 values equal to 0.9996 and 0.9917, RMSE values are 0.0013 and 0.0065 and MAE values of 0.0009 and 0.0033 for training and testing stages, respectively. Overall, the ANN models outperform the others in the testing stage with an R^2 value equal to 0.9957, RMSE value of 0.0044 and MAE value as 0.0017. Results of single factor analysis of variance (ANOVA) listed in Table 4 indicate there is no significant variation among the applied models. Figure 6 illustrates the agreement plots for actual and predicted values of various soft-computing-based models for the testing stages. Predicted discharge coefficient values using an ANN based model almost lie on the line of perfect agreement.

Table 5 displays the descriptive statistic of errors for the optimal data-intelligent models using the test period. According to Table 5, the ANN model generally follows the corresponding observed values for the lower, middle, and upper quartiles well. The other models have presented similar statistical distribution and the over/under estimation conditions are seen in some ranges.

The Taylor diagram of the observed and predicted C_d values from the different models under free flow conditions and for the test period is depicted in Figure 7. It is clear that the representative points of all models have nearly the same position. The ANN model (orange solid circle) is located nearest the observed value (hollow black circle) and this model adopted as the superior model.

Application of GP, SVM, ANN, GRNN, RF, and RT for estimating inclined gate submerged flow discharge coefficients (C_d)

For the performance evaluation of GP, SVM, ANN, GRNN, RF and RT based models for the prediction of discharge

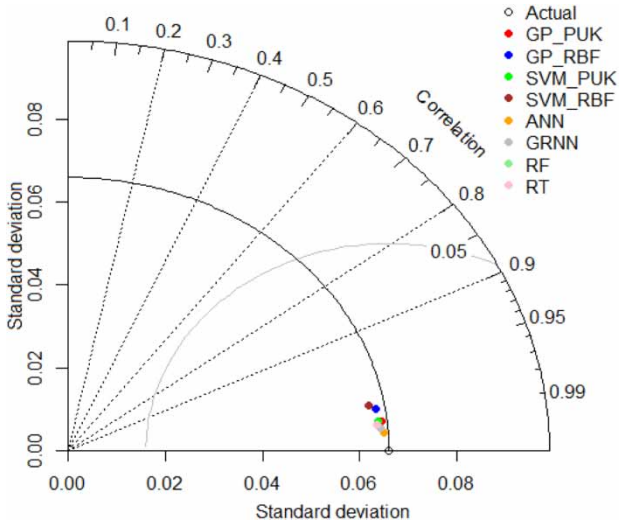

Figure 7 | Taylor plot for comparing the performance of models under free flow conditions. (Figure available in colour on line).

Table 5 | Statistics for error prediction related to C_d in free flow conditions

Statistic	GP_PUK	GP_RBF	SVM_PUK	SVM_RBF	ANN	GRNN	RF	RT
Minimum	−0.0420	−0.0560	−0.0500	−0.0710	−0.0250	−0.0383	−0.0430	−0.0370
Maximum	0.0090	0.0110	0.0040	0.0030	0.0060	0.0058	0.0070	0.0050
1st Quartile	−0.0010	−0.0050	−0.0008	−0.0020	−0.0010	−0.0003	−0.0020	−0.0030
3rd Quartile	0.0027	0.0060	0.0010	0.0020	0.0020	0.0007	0.0010	0.0010
Mean	0.0000	0.0002	−0.0012	−0.0034	0.0000	−0.0004	−0.0013	−0.0019

coefficients (C_d) in submerged flow, the same statistical parameters were used. The rate of y_t/a plays a key role along with y/a and β, and consequently was considered a model input. Table 6 depicts the comparison of performance evaluation parameters for the predicted discharge coefficient values. GP and SVM Pearson VII function-based universal kernel (PUK) based models work better than RBF kernel function-based models in the training and testing stages. GP based models work better than SVM based models for prediction of discharge coefficients in submerged flow conditions. The GRNN based model works better than the ANN based model in the model development stage whereas in the testing stage the ANN model works better than the GRNN model. Comparison of RF and RT based models (Table 6) suggest that the RF-based model works better than the RT-based model with R^2 value equal to 0.9724, RMSE value of 0.0163 and MAE value of 0.0082 for the testing stage. Overall, the ANN models outperform other models in the testing stage with an R^2 value of 0.9922, RMSE value of 0.0079, and MAE value of 0.0054. Results of single factor ANOVA listed in Table 7 suggests that there is no significant variation among the applied models. Figure 8 represents the agreement plots for actual and predicted values of the discharge coefficient.

Table 8 displays the descriptive statistics of errors for submerged flow conditions using test data. According to Table 8, the ANN model generally has well reproduced the corresponding observed values with lower minimum errors (−0.0180).

The Taylor diagram of the observed and predicted C_d values for different models with free flow conditions and for the test period is depicted by Figure 9. The representative

Table 6 | Comparison of statistical measures of C_d in submerged flow

	Training data set			Testing data set		
Models	**R^2**	**RMSE**	**MAE**	**R^2**	**RMSE**	**MAE**
GP_PUK	0.9795	0.0128	0.0072	0.9663	0.0163	0.0087
GP_RBF	0.9707	0.0153	0.0095	0.9558	0.0186	0.0110
SVM_PUK	0.9703	0.0171	0.0054	0.9552	0.0202	0.0076
SVM_RBF	0.9569	0.0209	0.0074	0.9359	0.0243	0.0099
ANN	0.9947	0.0066	0.0047	0.9922	0.0079	0.0054
GRNN	0.9994	0.0021	0.0009	0.9335	0.0234	0.0105
RF	0.9953	0.0072	0.0036	0.9724	0.0163	0.0082
RT	0.9997	0.0014	0.0008	0.9251	0.0263	0.0154

Table 7 | Single factor ANOVA results for the submerged flow condition

Source of variation	**F**	***P*-value**	**F crit**	**Variation in groups**
Between actual and GP_PUK	0.0101	0.9201	3.8613	Insignificant
Between actual and GP_RBF	0.0088	0.9251	3.8613	Insignificant
Between actual and SVM_PUK	0.1823	0.6696	3.8613	Insignificant
Between actual and SVM_RBF	0.3308	0.5655	3.8613	Insignificant
Between actual and ANN	0.0125	0.9112	3.8613	Insignificant
Between actual and GRNN	0.1318	0.7168	3.8613	Insignificant
Between actual and RF	0.0352	0.8514	3.8613	Insignificant
Between actual and RT	0.6688	0.4139	3.8613	Insignificant

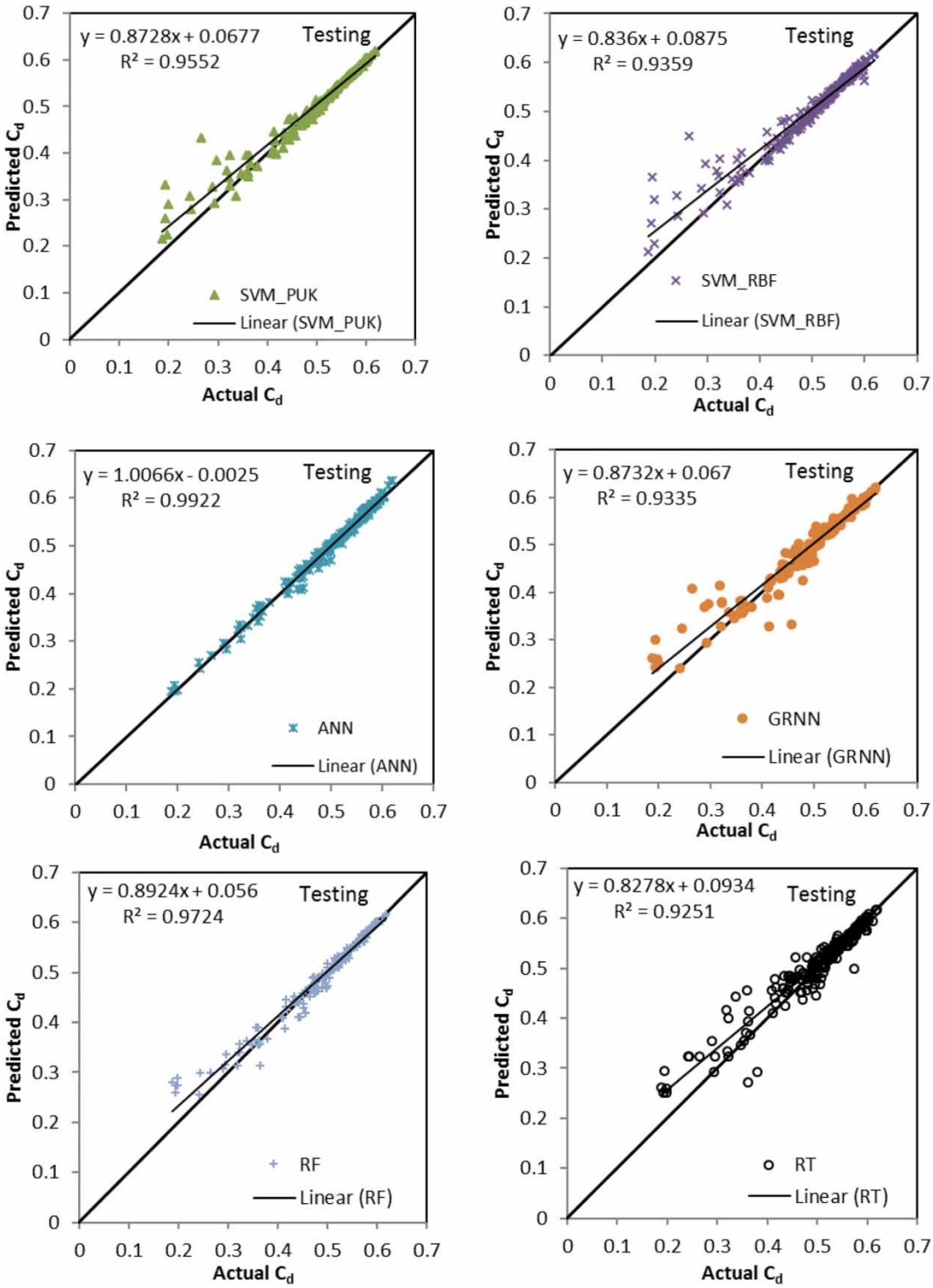

Figure 8 | Agreement plot for actual and predicted values of C_d in submerged flow using various soft computing techniques for the testing stage.

Table 8 | Descriptive error statistics for predicting C_d in free flow conditions

Statistic	GP_PUK	GP_RBF	SVM_PUK	SVM_RBF	ANN	GRNN	RF	RT
Minimum	−0.1280	−0.1360	−0.1670	−0.1850	−0.0180	−0.1437	−0.0930	−0.1070
Maximum	0.0330	0.0320	0.0290	0.0370	0.0350	0.1242	0.0520	0.0910
1st Quartile	−0.0040	−0.0060	−0.0010	−0.0030	−0.0053	−0.0028	−0.0030	−0.0110
3rd Quartile	0.0050	0.0080	0.0020	0.0040	0.0020	0.0023	0.0040	0.0040
Mean	−0.0008	−0.0007	−0.0033	−0.0043	−0.0009	−0.0028	−0.0014	−0.0062

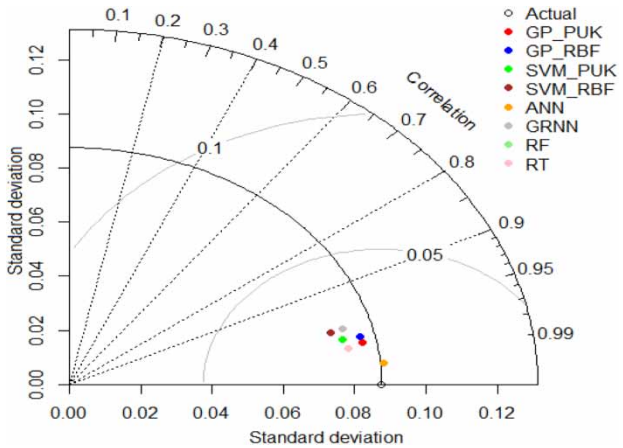

Figure 9 | Taylor plot for comparing the performance of applied models for submerged flow conditions. (Figure available in colour on line).

points from all applied models have nearly the same position; the ANN model (orange solid circle) is located nearest to the observed point (hollow black circle) and this model is introduced as the superior model.

CONCLUSIONS

The main purpose of the present study was to investigate inclined sluice gate discharge coefficients under free and submerged flow conditions. First, an inclined gate was created in a hydraulic laboratory at the University of Tabriz, in Iran. Considered variables were gate opening (a) and inclination angle (β) which included values of 0° (vertical gate), 15°, 30°, 45° and 60°. Experimental results showed the following:

1. Due to the convergence of flow lines under the gate, increasing the gate angle cause the discharge coefficient to increase.
2. Increasing the submergence ratio (y_t/a) causes a decrease in discharge coefficient values.
3. Increasing of submergence ratio causes a decline in discharge coefficients in both inclined and vertical gates, but the drop in discharge coefficients in vertical gates is greater than for inclined gates.

The GP, SVM, ANN, GRNN, RF, and RT based models were used for predicting the discharge coefficient (C_d) in both submerged and free flow conditions. According to the experimental results, 260 samples of free flow discharge and 741 samples of submerged discharge were used to evaluate the predictor models. The results show that:

1. in free flow conditions, the ANN model with $R^2 = 0.9957$, RMSE = 0.0044 and MAE = 0.0017 is the most accurate model compared to the other models in the testing stage;
2. in submerged flow conditions, the ANN models outperform the other models in the testing stage with $R^2 = 0.9922$, RMSE = 0.0079 and MAE = 0.0054.

For both submerged and free flow conditions, both GP and SVM based PUK models work better than RBF kernel based models in training and testing stages. For ANN and GRNN based models, the GRNN based models work better than ANN based models in the model development stage whereas in the testing stage the ANN model works better than GRNN based approach. Comparison of RF and RT based models suggest that the RF based model works better than the RT based model in both training and testing stages.

The results of the present study are confirmed by the results of Bijankhan & Ferro (2018). They used an inclined weir as the studied inclined gate. In that study, it was

found that increasing the weir inclination angle has positive effect on the weir discharge coefficient and the highest flow magnification ratio was 1.082.

CONFLICT OF INTEREST

The authors declare that they have no conflict of interest.

ACKNOWLEDGEMENTS

This research did not receive any specific grant from funding agencies in the public, commercial, or not-for-profit sectors.

ETHICAL APPROVAL

This article does not contain any studies with human participants or animals performed by any of the authors.

DATA AVAILABILITY STATEMENT

All relevant data are included in the paper or its Supplementary Information.

REFERENCES

Abdelhalim, F. S. F. 2016 Discharge estimation for submerged parallel radial gates. *Flow Measurement and Instrumentation* **52**, 240–245. https://doi.org/10.1016/j.flowmeasinst.2016.11.001.

Akbari, M., Salmasi, F., Arvanaghi, H., Karbasi, M. & Farsadizadeh, D. 2019 Application of gaussian process regression model to predict discharge coefficient of gated piano key weir. *Water Resources Management* **33** (11), 3929–3947. https://doi.org/10.1007/s11269-019-02343-3.

Al-Khatib, I. A. & Gogus, M. 2014 Prediction models for discharge estimation in rectangular compound broad-crested weirs. *Flow Measurement and Instrumentation* **36**, 1–8. https://doi.org/10.1016/j.flowmeasinst.2014.01.001.

Bahrami, B., Mohsenpour, S., Shamshiri Noghabi, H. R., Hemmati, N. & Tabzar, A. 2019 Estimation of flow rates of individual phases in an oil-gas-water multiphase flow system using neural network approach and pressure signal analysis. *Flow Measurement and Instrumentation* **66**, 8–23. https://doi.org/10.1016/j.flowmeasinst.2019.01.018.

Behar, O., Khellaf, A. & Mohammedi, K. 2015 Comparison of solar radiation models and their validation under Algerian climate-the case of direct irradiance. *Energy Conversion and Management* **98**, 236–251.

Belaud, G., Cassan, L. & Baume, J. P. 2009 Calculation of contraction coefficient under sluice gates and application to discharge measurement. *Journal of Hydraulic Engineering* **135** (12), 1086–1091.

Bijankhan, M. & Ferro, V. 2018 Experimental study and numerical simulation of inclined rectangular weirs. *Journal of Irrigation and Drainage Engineering* **144** (7), 04018012. https://doi.org/10.1061/(ASCE)IR.1943-4774.0001325.

Bijankhan, M. & Kouchakzadeh, S. 2014 The hydraulics of parallel sluice gates under low flow delivery condition. *Flow Measurement and Instrumentation*. http://dx.doi.org/10.1016/j.flowmeasinst.2014.10.017.

Bijankhan, M., Ferro, V. & Kouchakzadeh, S. 2013 New stage-discharge relationships for radial gates. *Journal of Irrigation and Drainage Engineering* **139**, 378–387. https://doi.org/10.1061/(ASCE)IR.1943-4774.0000556.

Brandhorst, N., Erdal, D. & Neuweiler, I. 2017 Soil moisture prediction with the ensemble Kalman filter: handling uncertainty of soil hydraulic parameters. Adv. *Water Resources* **110**, 360–370.

Breiman, L. 1999 *Random Forests*. UC Berkeley TR567.

Cassan, L. & Belaud, G. 2012 Experimental and numerical investigation of flow under sluice gates. *Journal of Hydraulic Engineering* **138**, 367–373. http://dx.doi.org/10.1061/(ASCE)HY.1943-7900.0000514.

Cios, K. J., Swiniarski, R. W., Pedrycz, W. & Kurgan, L. A. 2007 *The Knowledge Discovery Process*. Springer, Data Mining, pp. 9–24.

Cortes, C. & Vapnik, V. 1995 Support-vector networks. *Machine Learning* **20** (3), 273–297.

Daneshfaraz, R., Ghahramanzadeh, A., Ghaderi, A., Joudi, A. R. & Abraham, J. 2016 Investigation of the effect of edge shape on characteristics of flow under vertical gates. *American Water Works Association* **108** (8), E425–E431. http://dx.doi.org/10.5942/jawwa.2016.108.0102.

Gueymard, C. A. 2014 A review of validation methodologies and statistical performance indicators for modeled solar radiation data: towards a better bankability of solar projects. *Renewable and Sustainable Energy Reviews* **39**, 1024–1034.

Habibzadeh, A., Vatankhah, A. & Rajaratnam, N. 2011 Role of energy loss on discharge characteristics of sluice gates. *Journal of Hydraulic Engineering* **137** (9), 1079–1084. https://doi.org/10.1061/(ASCE)HY .1943-7900.0000406.

Henry, H. R. 1950 Discussion of 'Diffusion of submerged jets'. *Trans. Am. Soc. Civ. Eng.* **115**, 687–694.

Jahani, B. & Mohammadi, B. 2019 A comparison between the application of empirical and ANN methods for estimation of daily global solar radiation in Iran. *Theoretical and Applied Climatology* **137** (1–2), 1257–1269.

Jahanpanah, E., Khosravinia, P., Sanikhani, H. & Kisi, O. 2019 Estimation of discharge with free over fall in rectangular channel using artificial intelligence models. *Flow Measurement and Instrumentation* **67**, 118–130. https://doi.org/10.1016/j.flowmeasinst.2019.04.005.

Kalmegh, S. 2015 Analysis of Weka data mining algorithm REPTree, simple cart and random tree for classification of Indian news. *International Journal of Innovative Science, Engineering & Technology* **2** (2), 438–446.

Kang, F., Han, S., Salgado, R. & Li, J. 2015 System probabilistic stability analysis of soil slopes using Gaussian process regression with Latin hypercube sampling. *Computers and Geotechnics* **63**, 13–25. https://doi.org/10.1016/j.compgeo.2014.08.010.

Lorenzo, D., Mateos, L., Merkley, G. P. & Clemmens, A. J. 2009 Field calibration of submerged sluice gates in irrigation canals. *Journal of Irrigation and Drainage Engineering* **135** (6), 763–772. https://doi.org/10.1061/(ASCE)IR.1943-4774.0000085.

Maroufpoor, S., Maroufpoor, E., Bozorg Haddad, O., Shiri, J. & Yaseen, Z. M. 2019 Soil moisture simulation using hybrid artificial intelligent model: hybridization of adaptive neuro fuzzy inference system with grey wolf optimizer algorithm. *Journal of Hydrology.* **575** (2019), 544–556. https://doi.org/10.1016/j.jhydrol.2019.05.045.

Moazenzadeh, R. & Mohammadi, B. 2019 Assessment of bio-inspired meta-heuristic optimization algorithms for estimating soil temperature. *Geoderma* **353**, 152–171. https://doi.org/10.1016/j.geoderma.2019.06.028.

Norouzi, R., Daneshfaraz, R. & Ghaderi, A. 2019 Investigation of discharge coefficient of trapezoidal labyrinth weirs using artificial neural networks and support vector machines. *Applied Water Science.* **9**, 148. https://doi.org/10.1007/s13201-019-1026-5.

Nouri, M. & Hemmati, M. 2020 Discharge coefficient in the combined weir gate structure. *Flow Measurement and Instrumentation* **75**, 101780. https://doi.org/10.1016/j.flowmeasinst.2020.101780.

Parsaie, A., Azmathulla, H. M. & Haghiabi, A. H. 2017 Prediction of discharge coefficient of cylindrical weir–gate using GMDH-PSO. *ISH Journal of Hydraulic Engineering*. https://doi.org/10.1080/09715010.2017.1372226.

Parsaie, A., Haghiabi, A. H., Emamgholizadeh, S. & Azmathulla, H. M. 2019 Prediction of discharge coefficient of combined weir-gate using ANN. *ANFIS And SVM International Journal of Hydrology Science and Technology* **9** (4). https://doi.org/10.1504/IJHST.2019.102422

Rajaratnam, N. & Subramanya, K. 1967a Flow immediately below a submerged sluice gate. *Journal of Hydraulic Division* **93** (HY4), 57–77.

Rajaratnam, N. & Subramanya, K. 1967b Flow equation for the sluice gate. *Journal of Irrigation and Drainage Engineering* **93** (3), 167–186.

Ramamurthy, A. S., Submmanya, K. & Pani, B. S. 1978 Sluice gates with high discharge coefficients. journal of irrigation and drainage engineering. *ASCE* **104** (IR4), 437–441.

Roushangar, K., Akhgar, S. & Salmasi, F. 2017 Estimating discharge coefficient of stepped spillways under nappe and skimming flow regime using data driven approaches. *Flow Measurement and Instrumentation* **59** (2018), 79–87. https://doi.org/10.1016/j.flowmeasinst.2017.12.006.

Salmasi, F. & Nouri, M. 2017 Effect of upstream semi-impervious blanket of embankment dams on seepage. *ISH Journal of Hydraulic Engineering* **25** (2), 143–152. http://dx.doi.org/10.1080/09715010.2017.1381862.

Salmasi, F., Nouri, M. & Abraham, J. 2019 Laboratory study of the effect of sills on radial gate discharge coefficient. *KSCE Journal of Civil Engineering* **23**, 2117–2125. https://doi.org/10.1007/s12205-019-1114-y.

Seeger, M. 2004 Gaussian processes for machine learning. *International Journal of Neural Systems* **14** (02), 69–106.

Seyedzadeh, A., Maroufpoor, S., Shiri, J., Bozorg Haddad, O. & Gavazi, F. 2019 Artificial intelligence approach to estimate discharge of drip tape irrigation based on temperature and pressure. *Agricultural Water Management* **228**. https://doi.org/10.1016/j.agwat.2019.105905.

Shi, J. Q. & Choi, T. 2011 *Gaussian Process Regression Analysis for Functional Data*. CRC Press.

Shiri, J., Sadraddini, A. A., Nazemi, A. H., Marti, P., Fard, A. F., Kisi, O. & Landeras, G. 2015 Independent testing for assessing the calibration of the Hargreaves–Samani equation: new heuristic alternatives for Iran. *Computers and Electronics in Agriculture* **117**, 70–80.

Shiri, J., Nazemi, A. H., Sadraddini, A. A., Marti, P., Fard, A. F., Kisi, O. & Landeras, G. 2019 Alternative heuristics equations to the Priestley–Taylor approach: assessing reference evapotranspiration estimation. *Theoretical and Applied Climatology* **138** (1–2), 831–848.

Sihag, P. 2018 Prediction of unsaturated hydraulic conductivity using fuzzy logic and artificial neural network. *Modeling Earth Systems and Environment* **4** (1), 189–198. https://doi.org/10.1007/s40808-018-0434-0.

Silva, C. O. & Rijo, M. 2017 Flow rate measurements under sluice gates. *Journal of Irrigation and Drainage Engineering* **143** (6), 06017001. https://doi.org/10.1061/(ASCE)IR.1943- 4774.0001177.

Simon, H. 1999 *Neural Networks: A Comprehensive Foundation*. Prentice hall.

Specht, D. F. 1991 A general regression neural network. *IEEE Transactions on Neural Networks* **2** (6), 568–576.

Swamee, P. K. 1992 Sluice gate discharge equations. *Journal of Irrigation and Drainage Engineering* **118** (1), 56–60.

Swamee, P. K., Pathak, S., Mansoor, T., Shekhar, C. & Ojha, P. 2000 Discharge characteristics of skew sluice gates. *Journal of Irrigation and Drainage Engineering* **126** (5), 328–334. https://doi.org/10.1061/(ASCE)0733-9437(2000)126:5(328).

Vapnik, V., Golowich, S. E. & Smola, A. J. 1996 Support vector method for function approximation, regression estimation and signal processing. In: *Advances in Neural Information Processing systems 9 (NIPS 1996)*, pp. 281–287.

Wang, L. (ed.) 2005 Support Vector Machines: Theory and Applications. *Studies in Fuzziness and Soft Computing Vol. 177*, Springer Science & Business Media, Berlin, Heidelberg. https://doi.org/10.1007/b95439.

Wasserman, P. D. 1993 *Advanced Methods in Neural Computing*. John Wiley & Sons, Inc.

Williams, C. K. & Rasmussen, C. E. 2006 *Gaussian Processes for Machine Learning*, Vol. 2, No. 3. MIT Press, Cambridge, MA, p. 4.

Wu, S. & Rajaratnam, N. 2015 Solutions to rectangular sluice gate flow problems. *Journal of Irrigation and Drainage Engineering* **141** (12), 06015003. https://doi.org/10.1061/(ASCE) IR.1943-4774.0000922.

First received 18 June 2020; accepted in revised form 3 September 2020. Available online 18 September 2020